iScience

CellPress

Article

Plasticity of Synaptic Transmission in Human Stem Cell-Derived Neural Networks

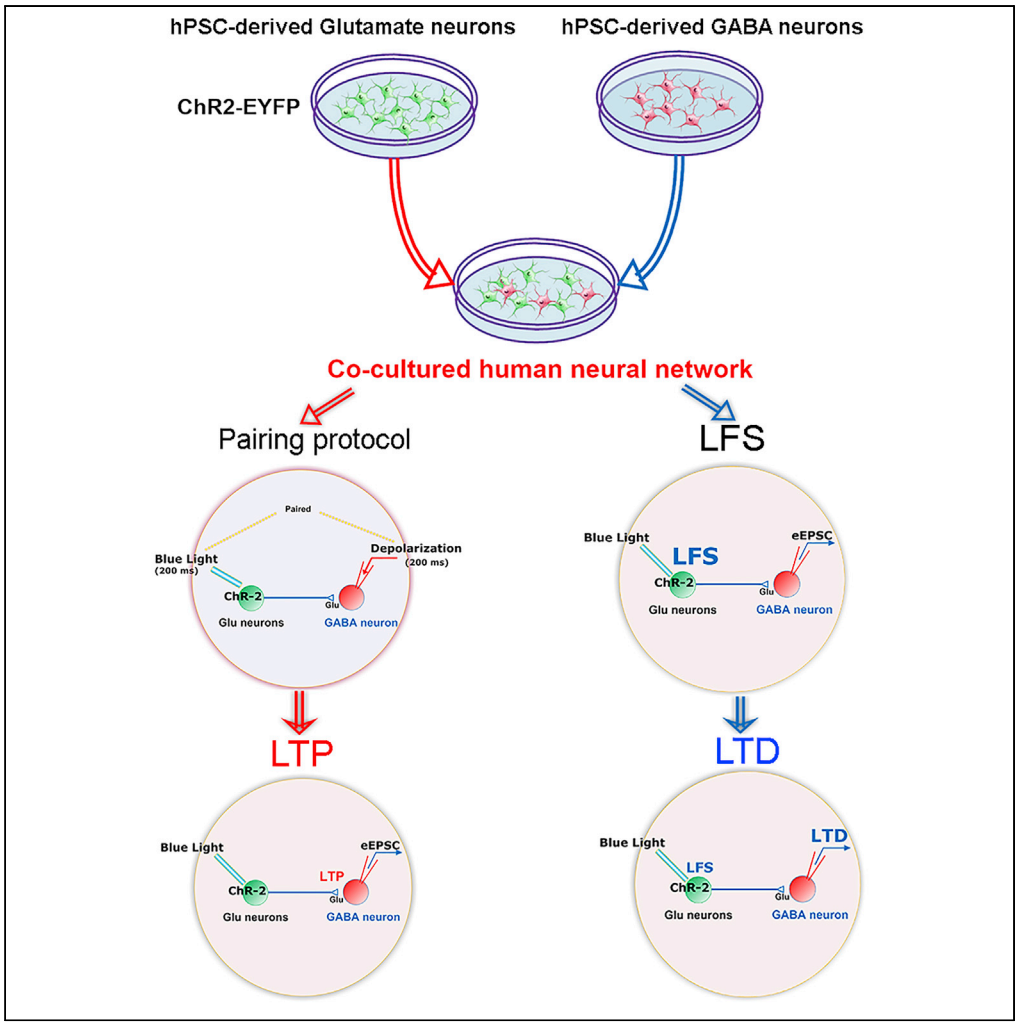

Yi Dong, Man Xiong, Yuejun Chen, Yezheng Tao, Xiang Li, Anita Bhattacharyya, Su-Chun Zhang

suchun.zhang@wisc.edu (S.-C.Z.)
brainstein@fudan.edu.cn (Y.D.)

HIGHLIGHTS

Repetitive stimulation induces LTP in hPSC-derived neural networks

Low-frequency light stimulation induces LTD in hPSCs-derived neural networks

The LTP/LTD in human neural networks are NMDAR dependent

Down syndrome neural networks exhibit defective LTP/LTD

Dong et al., iScience 23, 100829
February 21, 2020
https://doi.org/10.1016/j.isci.2020.100829

iScience

CellPress

Article

Plasticity of Synaptic Transmission in Human Stem Cell-Derived Neural Networks

Yi Dong,[1,2,3,8,*] Man Xiong,[6,8] Yuejun Chen,[3] Yezheng Tao,[3] Xiang Li,[3] Anita Bhattacharyya,[3] and Su-Chun Zhang[3,4,5,7,9,*]

SUMMARY

Long-term potentiation and depression, inferred from analysis on brain slices, are considered the cellular processes underlying learning and memory formation. They have not so far been demonstrated in human stem cell-derived neurons. By expressing channelrhodopsin in hESCs-derived glutamate neurons and co-culturing them with GABA neurons, we found that blue light stimulation increased the frequency of miniature excitatory postsynaptic currents (mEPSCs) and decreased the ratio of paired pulse facilitation (PPF) in non-ChR2-expressing GABA neurons, indicating a facilitating action at the presynaptic terminals. When paired with postsynaptic depolarization, the repetitive stimulation significantly increased the amplitude of light-evoked EPSCs that persisted during the period, indicating long-term potentiation (LTP). In contrast, low-frequency light stimulation induced long-term depression (LTD). These effects were blocked by N-methyl-D-aspartic acid (NMDA) receptor antagonists, suggesting NMDA receptor-mediated synaptic plasticity in human neural networks. Furthermore, induced pluripotent stem cell (iPSC)-derived neurons of patient with Down syndrome showed absence of LTP or LTD. Thus, our platform offers a versatile model for assessing human neural plasticity under physiological and pathological conditions.

INTRODUCTION

Learning and memory are mental activities formed through modifications of synaptic strength among simultaneously active neurons (Tang et al., 1999). The electrophysiological basis is long-term potentiation and long-term depression (LTP/LTD), two forms of activity-dependent synaptic plasticity (Bliss and Collingridge, 1993; Nabavi et al., 2014). Underlying the physiochemical changes are the activation of AMPA (α-amino-3-hydroxy-5-methyl-4-isoxazolepropionic acid) receptors followed by activation of postsynaptic N-methyl-D-aspartic acid (NMDA) receptors, which results in a rise in calcium concentration, a necessary trigger for LTP. Both presynaptic and postsynaptic neurons need to be stimulated simultaneously so that Ca^{2+} currents through the NMDA receptors are sufficient to activate the intracellular signaling cascades, including calmodulin-dependent protein kinase II (CaMKII), protein kinase C (PKC), and the tyrosine kinase Fyn (Dan and Poo, 2004), which ultimately alter the synaptic efficacy. Both LTP and LTD are best characterized in CA3 and CA1 glutamate neurons of the hippocampus in animals (Malenka, 1994), although they are also present in excitatory synapses in other brain regions, including the cerebral cortex, striatum, and amygdala (Daw et al., 2004; Lee and Kirkwood, 2011; Malenka and Bear, 2004; Sidorov et al., 2015; Suppa et al., 2015).

In humans, LTP/LTD is observed in surgically resected brain tissues (Beck et al., 2000; Chen et al., 1996). It is also observed indirectly through the long-lasting increase of the human auditory evoked potential or the rapid repetitive presentation of visual checkerboard-induced visual evoked potential (Clapp et al., 2005; Teyler et al., 2005). However, these are rare events and are difficult for mechanistic investigation. Given the availability of large collections of human stem cell lines, especially patient induced pluripotent stem cells (iPSCs), a simple and versatile model for analyzing the plasticity of human neuron networks will enable the understanding of changes in neural plasticity under physiological and pathological conditions.

We have engineered a simple yet versatile model for assessing neural plasticity by co-culturing channelrhodopsin (ChR2)-expressing glutamate neurons with non-ChR2-expressing GABA neurons, both of which are derived from human embryonic stem cells (ESCs). Repetitive light stimulation of glutamate neurons paired with postsynaptic depolarization persistently increased the amplitude of light-evoked EPSCs recorded in the GABA neurons, exhibiting LTP-like behavior. In contrast, low-frequency light stimulation

[1]Key Laboratory of Adolescent Health Assessment and Exercise Intervention of Ministry of Education, East China Normal University, Shanghai 200241, China

[2]School of Physical Education & Health Care, East China Normal University, Shanghai 200241, China

[3]Waisman Center, University of Wisconsin, Madison, WI 53705, USA

[4]Department of Neuroscience, School of Medicine and Public Health, University of Wisconsin, Madison, WI 53705, USA

[5]Department of Neurology, School of Medicine and Public Health, University of Wisconsin, Madison, WI 53705, USA

[6]Institute of Pediatrics, Children's Hospital, Fudan University, 399 Wanyuan Road, Shanghai 201102, China

[7]Program in Neuroscience & Behavioral Disorders, Duke-NUS Medical School, Singapore, Singapore

[8]These authors contributed equally

[9]Lead Contact

*Correspondence: suchun.zhang@wisc.edu (S.-C.Z.), brainstein@fudan.edu.cn (Y.D.)

https://doi.org/10.1016/j.isci.2020.100829

decreased the amplitude of light-evoked EPSCs, signaling LTD. When the ChR2-glutamate neurons are from Down syndrome (DS) patient iPSCs, LTP/LTD was not induced.

RESULTS

Stimulation of Glutamate Neurons Potentiates the Frequency of mEPSCs in GABA Neurons

To enable precise stimulation of presynaptic neurons we established a ChR2-expressing human embryonic stem cells (hESC) line by inserting ChR2 and EYFP (for identification) in the AAVS1 locus under the CAG promoter by CRISPR (clustered regularly interspaced short palindromic repeats, Figure S1A). Genomic PCR confirmed the integration of the transgene in the resulting clonal hESCs (Figure S1B). Homozygous clones with two copies of the ChR2 gene were selected (Figure S1B). The ChR2-EYFP-expressing hESCs were differentiated to glutamatergic neurons (Li et al., 2009) in the presence of sonic hedgehog antagonist cyclopamine with 92.9 $\pm$ 3.3% of the total cells expressing glutamine synthase at day 36 (Figure S1D). The non-ChR2 hESCs were differentiated to medial ganglionic eminence progenitors and then to GABAergic neurons (Liu et al., 2013) with 81.9 $\pm$ 2.3% of total cells positive for GABA (Figure S1E). The ChR2-expressing cortical glutamate neurons were then co-cultured with cortical GABA interneurons derived from non-ChR2-expressing hESCs at a ratio of 2:1 (Figure 1A). Immunostaining of the co-cultures indicated that almost all the cells express a forebrain marker OTX2 but not the hippocampal marker Prox1 (Figures S1C and S1H), indicating the forebrain identity of the cells. The cultures were maintained for 5–7 weeks before recording.

By plotting peak membrane potential (MP) response on current injection without action potential (AP) occurrence, the membrane input resistance (Rin) is 78.13 $\pm$ 3.43 MΩ (n = 7). The resting membrane potential is 58.25 $\pm$ 6.35 mV (n = 7). Under the blue light stimulation (2 s, 470 nm, 0.4 mW/mm^2), robust action potentials (APs) were elicited in the glutamate neurons under the current-clamp mode (12.5 $\pm$ 0.49 Hz, n = 7, Figure S1F[1] [2]). In the voltage-clamp mode, at a holding potential of −70 mV, the same light stimulation elicited large inward currents with action currents (n = 7, Figure S1F[3]). Treatment with 1 μM tetrodotoxin (TTX) eliminated the action currents, suggesting that the remaining currents are ChR2-induced currents with two components: a large current with fast decay kinetics and a steady-state current (122.87 $\pm$ 8.79 pA at peak and 55.09 $\pm$ 2.65 pA at steady state, n = 7, Figure S1F[4]). Light stimulation had no effect on the GABA neurons that were differentiated from the non ChR2-expressing hESCs. Together, these data suggest that ChR2 is expressed in hESC-derived glutamatergic neurons and can induce rapid physiological responses with high fidelity and low "noise."

We then evaluated synaptic interactions between the ChR2-expressing cortical glutamate neurons and the non-ChR2-expressing cortical GABA neurons. The recording GABA neurons were first identified as non-fluorescent and non-responsive to light stimulation. GABA neurons had spontaneous action potentials, often with a "fast-spiking" pattern (Figure S1G[1]). The spikes of GABA neurons were narrower than those of glutamate neurons and had a sharper repolarization (Figure S1G[2]), consistent with the findings in mouse neurons (Bean, 2007). After recording, we verified the identity by their positive staining for GABA (Figure S1G[1] left panel).

Before light stimulation of the glutamatergic neurons, the mean frequency of miniature excitatory postsynaptic currents (mEPSCs) in GABA neurons was 2.53 $\pm$ 0.52 Hz (n = 8), suggesting a high degree of connectivity. mEPSCs were abolished by the AMPA receptor antagonist NBQX (20 μM). With blue light (60 s, 470 nm, 0.4 mW/mm^2) stimulation, the mean frequency of mEPSCs in GABA neurons increased to 5.19 $\pm$ 1.08 Hz. The effect reached statistical significance during the stimulation (range, 60–120 s, $p < 0.05$, n = 8, versus before, Figure 1B) and was not accompanied by changes in mEPSC amplitude. Following the light stimulation (180–240 s), the frequency of mEPSCs recovered to 3.18 $\pm$ 0.45 Hz ($p > 0.05$, n = 8, versus before) (Figures 1C and 1E). This is also illustrated by the cumulative distribution of the inter-event intervals of mEPSCs during light stimulation, showing a leftward shift, or a shorter inter-event interval, compared with the control and post-light stimulation (Figure 1D, $p < 0.01$; Kolmogorov-Smirnov test). Thus, light stimulation of the ChR2-expressing glutamatergic neurons potentiates the frequency of mEPSCs recorded in GABA neurons. To further demonstrate a facilitating action at the presynaptic terminals, we recorded PPF (paired pulse facilitation) at the presynaptic site in response to light stimulation. As shown in Figure 1F, light stimulation decreased the PPF ratio (P2/P1) from 1.4 $\pm$ 0.02 to 1.22 $\pm$ 0.04 (n = 6, $p < 0.05$). Together, these results suggest that light stimulation of the ChR2-expressing glutamatergic neurons potentiates the presynaptic glutamate release to GABA neurons.

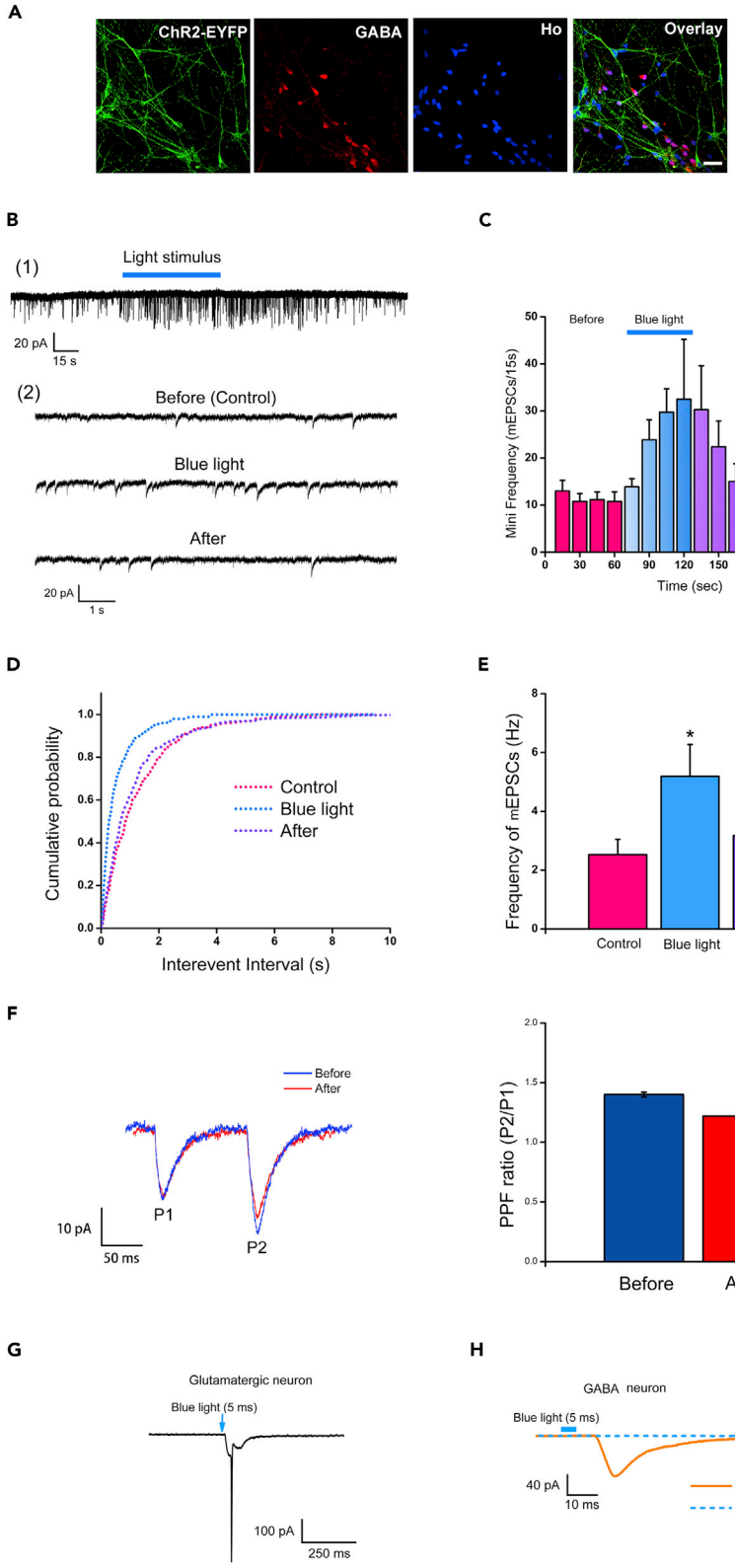
A
ChR2-EYFP
GABA
Ho
Overlay
B
(1)
Light stimulus
20 pA
15 s
(2)
Before (Control)
Blue light
After
20 pA
1 s
C
Before
Blue light
After
Mini Frequency (mEPSCs/15s)
Time (sec)
D
Cumulative probability
Control
Blue light
After
Interevent Interval (s)
E
Frequency of mEPSCs (Hz)
Control
Blue light
After
F
Before
After
P1
P2
10 pA
50 ms
PPF ratio (P2/P1)
Before
After
G
Glutamatergic neuron
Blue light (5 ms)
100 pA
250 ms
H
GABA neuron
Blue light (5 ms)
40 pA
10 ms
eEPSC
NBQX

Figure 1. Effect of Light Stimulation on the Frequency of mEPSCs in non-ChR2-expressing GABA Neurons

(A) Immunostaining of co-cultures of forebrain glutamate neurons derived from ChR2-EYFP-expressing hESCs and GABA neurons derived from wild-type hESCs at 5 weeks after plating. Ho, Hoechst. Scale bar, 25 μm.

(B) Representative mEPSCs of a GABA neuron before, during, and after the light stimulation. (1) The 4 min of recording of mEPSCs. (2) Expanded timescale of the mEPSC recording before, during, and after the light stimulation.

(C) Time course of the average number of mEPSCs before, during, and after the light stimulation (the bin size is 15 s) (n = 8, mean ± SEM).

(D) The cumulative distributions of the inter-event intervals of mEPSCs before, during, and after the light stimulation.

(E) The averaged mEPSC frequency in GABA neurons before, during, and after the light stimulation (mean ± SEM, n = 8, paired t test, versus before [control]).

(F) Effect of light stimulation on PPF in non ChR2-expressing GABA neurons. Left, typical recordings of PPF before and after light stimulation. Holding potential, −70 mV. Right, Averaged PPF before and after light stimulation ($p < 0.05$, n = 6, mean ± SEM, t test).

(G) The action currents triggered by 5-ms pulses of blue light in ChR2-expressing glutamate neurons under voltage-clamp mode.

(H) eEPSC recording in a non-ChR2-expressing GABA neuron.

Besides presynaptic regulation, postsynaptic response is similarly important for regulating synaptic transmission. Under pulse stimulation of blue light (5 ms), action currents were triggered in ChR2-expressing glutamatergic neurons under the voltage-clamp mode (Figure 1G). At the holding potential of −70 mV with extracellular Mg^{2+} concentration of 2 mM, which blocks NMDA receptor-mediated currents, the pulse blue light stimulation induced a large evoked EPSC (eEPSC, ~70pA) in postsynaptic GABA neurons (Figure 1H). The interval between the blue light stimulus and the postsynaptic potential is 6.87 ± 0.05 ms. The eEPSC was completely inhibited by the AMPA receptor antagonist NBQX (2,3-dihydroxy-6-nitro-7-sulfamoyl-benzo[f]quinoxaline-2,3-dione, 20 μM, Figure 1H), suggesting that the eEPSC was induced by the presynaptic glutamatergic release and mediated by the activation of AMPA receptors in postsynaptic GABA neurons. Together, light stimulation regulates presynaptic release, which in turn evokes strong postsynaptic response, enabling regulation of synaptic transmission.

Repetitive Light Stimulation Induces LTP

With the ability to regulate synaptic transmission between cultured human neurons by light stimulation, we asked if it is possible to induce LTP between presynaptic glutamatergic neurons and postsynaptic GABA neurons. The typical protocol for LTP induction in brain slices involves high-frequency electric stimulation of presynaptic action potentials paired with postsynaptic depolarization (Chen et al., 1999). We have designed a new light-induction protocol consisting of a 200 ms light stimulation of ChR2-expressing glutamatergic neurons paired with postsynaptic depolarization (voltage step to 0 mV, 200 ms) of the patch-clamped GABA neuron (Figure 2A). Pairing was repeated 20 times at 0.1 Hz (Figure 2B). After the pairing protocol, the holding voltage was rapidly restored to −70 mV, thus establishing a stable baseline for eEPSC induction. Upon light stimulation, the eEPSC amplitudes increased significantly (Figure 2C top), from 70.36 ± 7.46 pA before to 134.74 ± 16.91 pA after the pairing protocol ($p < 0.05$, n = 13, Figure 2D). On average, the eEPSC amplitude was potentiated to 191.50 ± 24.61% of the control amplitude ($p < 0.05$, n = 13, Figure 2F). The increase in eEPSC amplitude persisted throughout the duration (30 min) of the recording (Figures 2D and 2E), indicating an LTP-like behavior. Besides the amplitude, the frequency of mEPSCs increased from 2.14 ± 0.46 to 4.31 ± 0.52 Hz after the LTP protocol ($p < 0.05$, n = 6, Figure 2G), indicating the increase in presynaptic glutamate release. Among the 59 GABA neurons that were responsive to light stimulation, i.e., synaptically connected (each from a different dish), 13 exhibited LTP-like behavior using our pairing protocol (22%).

To examine the mechanism underlying the potentiation, we applied AP-5 (amino-5-phosphonovaleric acid), an NMDA receptor antagonist, during the paired recording. The presence of AP-5 (50 μM) completely blocked the potentiation of eEPSCs (65.69 ± 6.44 pA before versus 63.16 ± 5.98 pA during pairing in the presence of AP-5, $p > 0.05$, n = 14, Figures 2C bottom, and 2D–2F), suggesting an NMDA receptor-dependent event.

Low-Frequency Stimulation Induces LTD

Another form of synaptic plasticity is LTD. LTD is typically induced by low-frequency stimulation (LFS). We thus evaluated LTD in the above co-culture system by stimulating the ChR2-expressing glutamate neurons with low frequency (900 pulse, 3 Hz) of blue light and recording the non-ChR2-expressing GABA neurons.

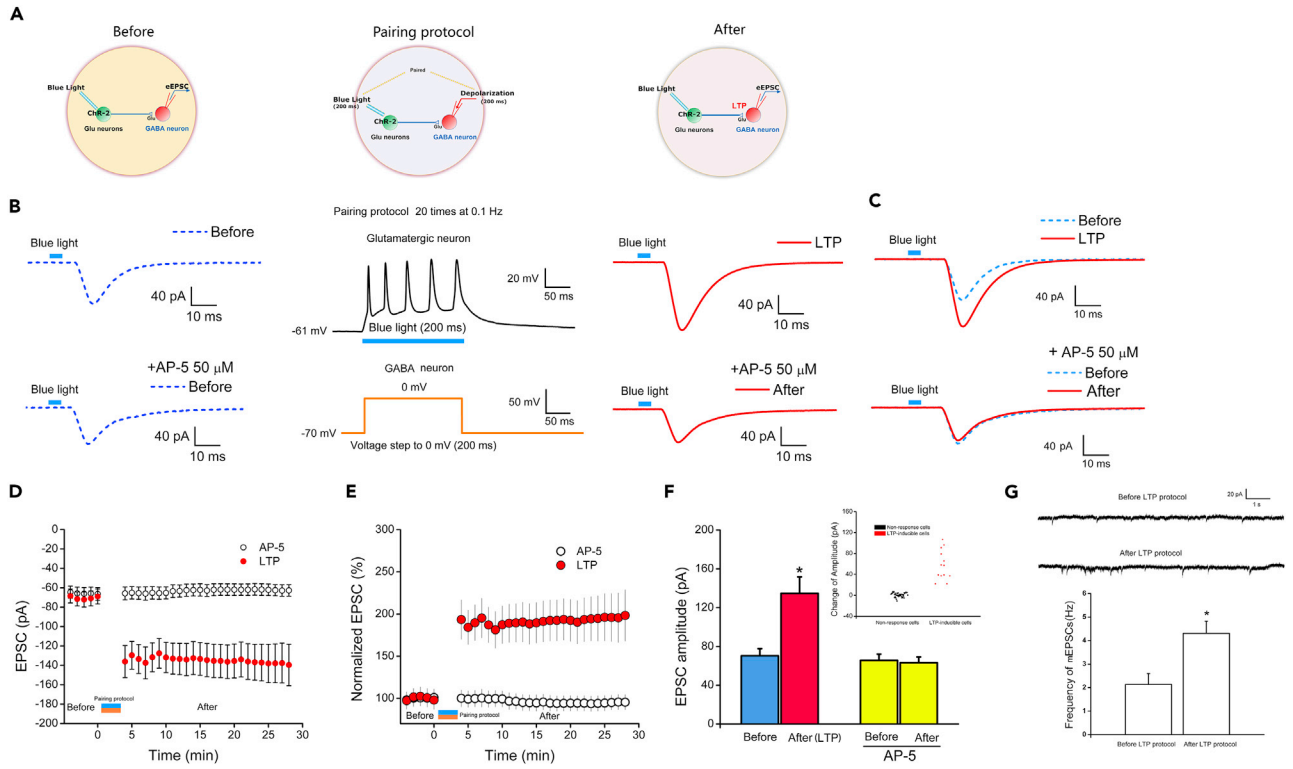

Figure 2. Induction of LTP in Cultured Human Neurons

(A) Cartoon of LTP induction. Left panel: blue light stimulates the ChR2-expressing glutamate neurons while recording eEPSCs in GABA neurons before pairing protocol. Middle panel: pairing protocol. Right panel: continued recording of eEPSC after pairing protocol.

(B) LTP induction protocol in the co-culture system. Five action potentials are induced by blue light stimulation (200 ms) of the ChR2-expressing glutamate neurons (Upper) when paired with a postsynaptic depolarization (voltage step to 0 mV, 200 ms) of the patch-clamped GABA neuron (Bottom). The protocol was repeated 20 times at 0.1 Hz.

(C) Raw traces of an eEPSC recorded in a non ChR2-expressing GABA neuron. Top panel: raw traces before and after pairing protocol stimulation. Bottom panel: raw traces before and after pairing protocol stimulation in the presence of AP-5.

(D) Change in the amplitude of light-evoked EPSCs before and after pairing protocol in the absence and presence of AP-5 over 30-min recording.

(E) The percentage increase of light-evoked EPSCs before and after pairing protocol in the absence and presence of AP-5.

(F) Averaged amplitude of eEPSCs before and after pairing protocol in the absence ($p < 0.05$, n = 13, mean ± SEM, t test) and presence of AP-5 ($p > 0.05$, n = 14, mean ± SEM, t test). Inset: Full distribution of the change of eEPSC amplitude from 59 cells studied in the LTP-like protocol.

(G) The effect of LTP protocols on the frequency of mEPSCs in non ChR2-expressing GABA neurons. Upper, representative mEPSCs of a GABA neuron before and after the LTP protocol. Bottom, the averaged mEPSC frequency in GABA neurons before and after the LTP protocol ($p < 0.05$, n = 6, mean ± SEM, t test).

Under this condition, the eEPSC amplitudes decreased significantly, from 73.43 ± 6.32 pA before to 56.56 ± 8.27 pA after the LFS protocol ($p < 0.05$, n = 9, Figures 3A, 3B, and 3D). The normalized eEPSC amplitude was decreased to 77.02 ± 11.46% of the control ($p < 0.05$, n = 9, Figure 3C). The decrease in both the absolute value and the percentage change of eEPSC amplitude persisted throughout the duration (30 min) of the recording (Figures 3B and 3C), indicating an LTD-like behavior. In addition, the frequency of mEPSCs decreased from 2.51 ± 0.25 to 1.38 ± 0.21 Hz after the LTD protocol ($p < 0.05$, n = 6, Figure 3E), indicating the decrease in presynaptic glutamate release. Among the 26 synaptically connected GABA neurons, 9 exhibited LTD (35%, each from a different dish, Figure 3D inset). Again, blockade of NMDA receptors with AP-5 prevented the LTD (67.03 ± 2.47 pA before versus 68.33 ± 5.6 pA after stimulation, $p > 0.05$, n = 14, Figures 3B, 3C, and 3D), suggesting NMDA receptor-dependent LTD formation.

LTP/LTD Induction Is Accompanied by Molecular Changes in Postsynaptic Cells

Molecular analysis on acutely prepared rodent brain slices following electrophysiological stimulation and recording has identified several signaling molecules to be differentially regulated at the transcriptional level accompanying the change of the postsynaptic strength (Nicoll, 2017). These include

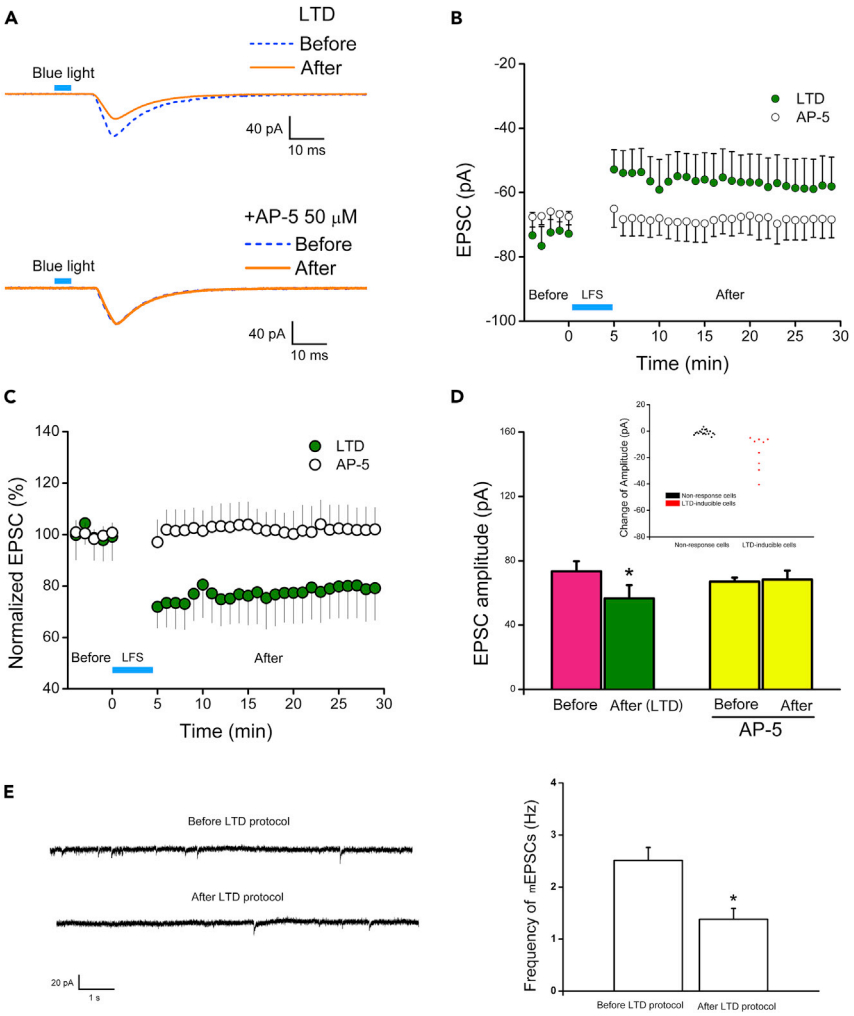

Figure 3. Induction of LTD in Human Neurons

(A) Raw traces of eEPSCs recorded in a non-ChR2-expressing GABA neuron. Top panel: raw traces before and after LFS. Bottom panel: raw traces before and after LFS in the presence of AP-5.

(B) The amplitude of light-evoked EPSCs before and after LFS in the absence and presence of AP-5 during the 30-min recording.

(C) Time course of changes in percentage of eEPSCs before and after LFS in the absence and presence of AP-5.

(D) Averaged amplitude of eEPSCs before and after LFS in the absence ($p < 0.05$, $n = 9$, mean ± SEM, t test) and presence of AP-5 ($p > 0.05$, $n = 14$). Inset: Full distribution of the change of eEPSC amplitude from 26 cells studied in the LTD protocol.

(E) The effect of LTD protocols on the frequency of mEPSCs in non ChR2-expressing GABA neurons. Left, representative mEPSCs of a GABA neuron before and after the LTD protocol. Right, the averaged mEPSC frequency in GABA neurons before and after the LTD protocol ($p < 0.05$, $n = 6$, mean ± SEM, t test).

Ca^{2+}/calmodulin-dependent protein kinase II (CAMKII) that plays the key role in the induction and maintenance of the long-term synaptic dynamic (Kim et al., 2016) and immediate-early genes (IEGs) that are activated following synaptic activation, including the inducible transcription factors (ITF) c-FOS (FOS), ZIF268 (EGR1), and CREB (CREB1) (Li et al., 2017; Minatohara et al., 2015). To determine if induction of LTP and LTD in our cultured human neurons is accompanied by similar molecular changes in the postsynaptic neurons to those observed in rodent brain slices, we aspirated off the intracellular components and performed single cell PCR assay. Strikingly, the expression level of CAMKII increased by 5-fold in cells after LTP induction compared with those synaptically connected but without LTP induction (Figure S2A left panel). In contrast, CAMKII decreased by-9 fold after LTD (Figure S2A right panel). IEGs, including c-FOS, EGR1, and CREB1, significantly increased after LTP induction but decreased after LTD except

that the reduction in EGR1 expression was not statistically significant (Figure S2B). We further measured calcium influx at the presynaptic site in response to light stimulation, showing an increase in fluorescein intensity (IOD: 100 ± 10.99% before versus 203.52 ± 11.75% after, n = 4, $p < 0.001$) and area (100 ± 12.4% before versus 191.06 ± 11.49% after, n = 4, $p < 0.001$) (Figure S2C). Together, these results suggest that light stimulation of the ChR2-expressing glutamatergic neurons potentiates the presynaptic glutamate release to GABA neurons. They also suggest that the synaptic dynamics in our *in vitro* human neuronal network shares similar molecular processes to those revealed by *ex vivo* brain slices.

Down Syndrome Patient iPSC-Derived Neurons Show Absence of LTP/LTD

The ability to measure LTP and LTD from human stem cell-derived neuronal networks opens a possibility to interrogate if neuronal networks from patients with neurological and psychiatric disorders are altered. We have previously shown that cortical neurons derived from iPSCs of DS, a common developmental disease with mental retardation caused by an extra chromosome 21, show reduced synaptic currents (Weick et al., 2013). To validate the utility of our assay in iPSC-derived neuronal networks and to determine if DS cortical neurons exhibit defective LTP/LTD, we expressed ChR2-EYFP in DS patient iPSCs or isogenic control iPSCs by CRISPR and then co-cultured the ChR2-EYFP glutamate neurons (from DS or isogenic control iPSCs) with non-ChR2 GABA neurons (from H9 ESCs) by 2:1 (Figure 4A), similar to the ratio for non-DS cells mentioned above.

Following the same LTP-induction protocol described above, we found that, in the isogenic control group, the eEPSC amplitudes changed significantly, from 70.48 ± 3.38 pA before to 103.64 ± 10.64 pA ($p < 0.05$, n = 7 [of 34 connected cells], Figure 4B) after the same light stimulation protocol. On average, the eEPSC amplitude was potentiated to 139.20 ± 14.44% of the control amplitude (Figure 4D). The increase in eEPSC amplitude also persisted throughout the duration (30 min) of the recording (Figures 4C and 4D), indicating an LTP-like behavior. Among the 34 neurons that were responsive to light stimulation, i.e., synaptically connected, 7 exhibited LTP-like behavior using our pairing protocol (20.5%), indicating that our protocol is reproduced in iPSC-derived neurons with a similar efficiency. In contrast, among the 16 DS iPSC-derived neurons that were responsive to light stimulation, i.e., synaptically connected (each from a different dish), none exhibited LTP-like behavior (0%). The eEPSCs in DS patient iPSC-derived neural network did not show obvious changes (74.30 ± 2.55 pA before versus 71.78 ± 3.01 pA after the LTP-induction protocol, $p > 0.05$, n = 16, Figures 4B, 4C, and 4D), indicating an absence of LTP.

We then asked if LTD is affected in DS neurons. Under the same LTD-induction condition described above, we found that the eEPSC amplitudes decreased significantly in the isogenic group, from 70.10 ± 2.67 pA before to 52.70 ± 4.61 pA ($p < 0.05$, n = 4 [of 12 connected cells], Figure 4E) after the same LFS protocol. On average, the eEPSC amplitude was decreased to 79.32 ± 6.14% of the control amplitude (Figure 4G). The decrease in eEPSC amplitude also persisted throughout the duration (30 min) of the recording (Figures 4F and 4G), indicating an LTD-like behavior. Among the 12 neurons that were responsive to light stimulation, i.e., synaptically connected, 4 exhibited LTD-like behavior (33.3%), indicating that LTD is replicated in isogenic iPSC-derived neurons with a similar efficiency. In contrast, in the DS group, none exhibited LTD-like behavior (0%) among the eight neurons that were responsive to light stimulation, i.e., synaptically connected (each from a different dish). The eEPSCs in DS patient iPSC-derived neural network did not show obvious changes (67.84 ± 3.01 pA before versus 64.51 ± 2.96 pA after the LFS protocol, $p > 0.05$, n = 8, Figure 4E), signaling the lack of LTD induction.

DISCUSSION

We have created a platform to enable analysis of neural plasticity in cultured human neurons. This is made possible by co-culturing hESC-derived inhibitory (GABA) neurons with excitatory (glutamate) neurons that are engineered with an optogenetic control (Ge et al., 2006; Li et al., 2012; Steinbeck et al., 2015; Weick et al., 2011). With such a model, we have now shown that LTP and LTD can be efficiently elicited in human neuronal networks by precisely regulating the activity of excitatory neurons and that the induction of LTP/LTD is NMDA receptor dependent. This assay is reproduced using iPSC-derived neuronal networks and in different laboratories. Furthermore, we found that LTP/LTD induction is defective in DS iPSC-derived cortical neuronal networks, highlighting the utility of such an *in vitro* platform for examining the plasticity of human neural networks under physiological and pathological conditions.

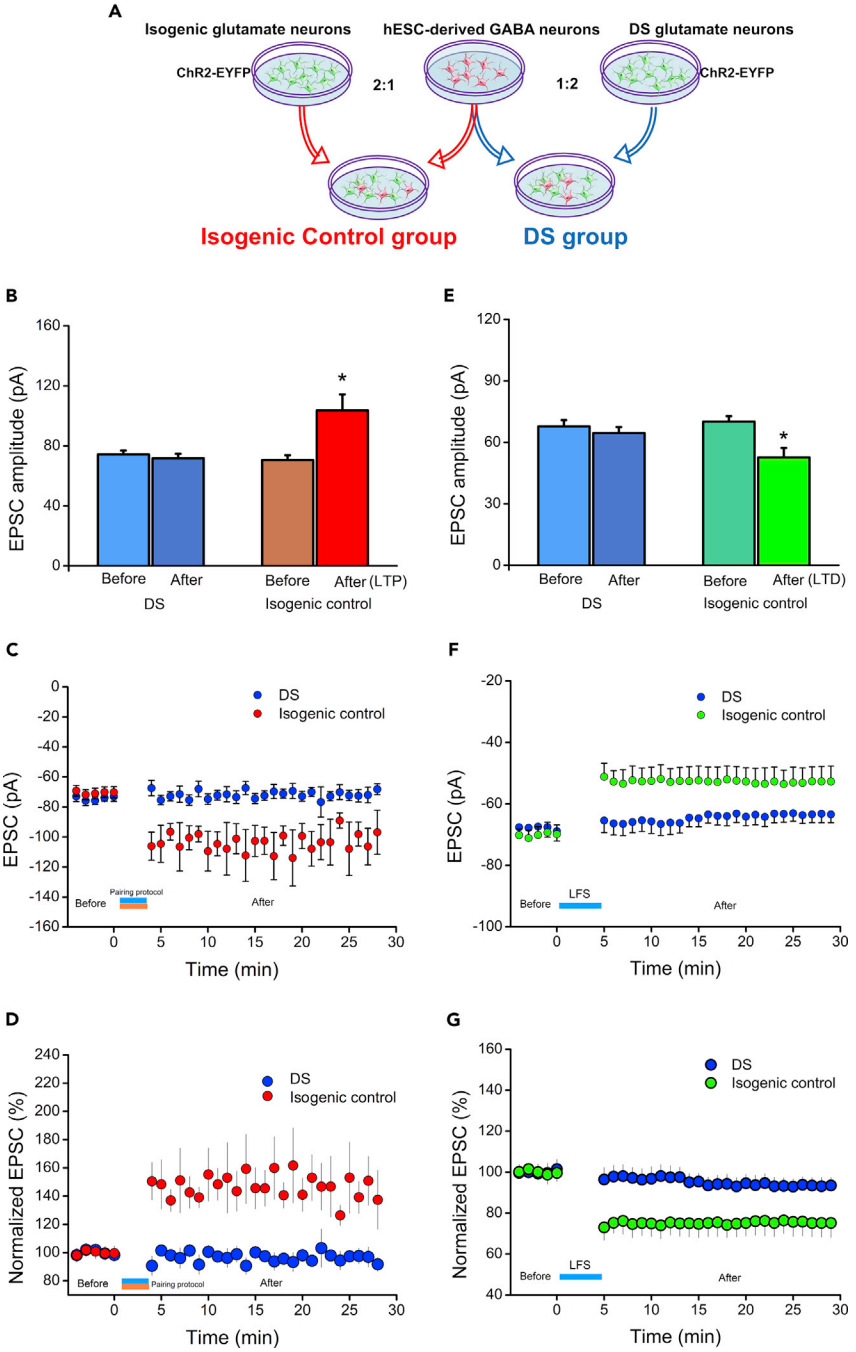

Figure 4. Induction of LTP/LTD in DS Patient iPSC- and Isogenic iPSC-Derived Neural Networks

(A) Cartoon of the co-culture between DS/isogenic glutamate neurons and hESC-derived GABA neurons.

(B) Averaged amplitude of eEPSCs before and after pairing protocol in DS patient iPSC- ($p > 0.05$, n = 16, mean ± SEM, t test) and isogenic iPSC-derived neural network ($p < 0.05$, n = 7, mean ± SEM, t test).

(C) Change in the amplitude of light-evoked EPSCs before and after pairing protocol over 30-min recording.

(D) The percentage increase of light-evoked EPSCs before and after pairing protocol.

(E) Averaged amplitude of eEPSCs before and after LFS in DS patient iPSC- ($p > 0.05$, n = 8, mean ± SEM, t test) and isogenic iPSC-derived neural network ($p < 0.05$, n = 4, mean ± SEM, t test).

(F) Change in the amplitude of light-evoked EPSCs before and after LFS over 30-min recording.

(G) The percentage decrease of light-evoked EPSCs before and after LFS.

LTP/LTD is measured by stimulating the presynaptic components with electric stimulation and recording changes of synaptic strength at the postsynaptic end typically in well-defined structures, such as the hippocampus (Bliss and Collingridge, 2013). Even so, recording of LTP/LTD remains a rare event experimentally (Buonomano and Merzenich, 1998; Chen et al., 1994). It is nearly impossible to induce direct LTP/LTD in cultured neurons because the electric stimulation only activates the adjacent neurons owing to the attenuation of an electric field. Because of these difficulties, the change in mEPSC amplitude in cultured mouse hippocampal neurons is used to replace the evoked EPSCs in slices (Lu et al., 2001; Man et al., 2003; Ninan et al., 2006). Such a low efficiency places a substantial technical burden on recording LTP/LTD in "randomly" connected human neurons. In addition, electric stimulation activates both presynaptic and postsynaptic neurons at the same time because of the randomness in co-cultured neural circuits, making it difficult to interpret results. To overcome these technical hurdles, we have established a ChR2-expressing hESC line by CRISPR so that the activity of the derived neurons can be precisely regulated. Indeed, expression of ChR2 enables not only precise regulation of presynaptic human neuronal activity but also postsynaptic neuronal response (Weick et al., 2011). More importantly, simultaneous stimulation of large numbers of presynaptic glutamate neurons not only increases the probability of synaptic inputs but also synchronizes the inputs onto the recording postsynaptic neurons, thus amplifying outputs. Such a strategy enables us to achieve LTP/LTD in a substantial proportion (20%–30%) of synaptically connected neurons.

Induction of LTP/LTD requires coordinated changes at both the pre- and postsynaptic ends. After series of testing, we have identified a set of light-stimulation parameters that can effectively alter the strength of the presynaptic release. In particular, the repetitive light stimulation (200-ms light stimulation pairing with postsynaptic depolarization 20 times at 0.1 Hz) augments the presynaptic release of glutamate, as indicated by increased amplitude and frequency of eEPSCs, elevated calcium influx, and increased expression of CAMKIIA. This is very much similar to the changes induced by HFS in brain slices (Sokolov et al., 2003). When coupled with postsynaptic depolarization, it effectively induces LTP. The changes at the postsynaptic end induced by light stimulation are also similar to those seen in brain slices induced by electric stimulation, including changes of activity-regulated genes (immediate-early genes) like FOS, EGR1, and CREB1. These genes are preferentially expressed in the neurons that encode long-term memory in rodent models and are thought to be the markers of the memory engram (Liu et al., 2014; Zhou et al., 2009). Interestingly, the expression level of CAMKIIA in our postsynaptic human GABA neurons is also positively correlated with the neural activity, similar to a previous report using rodents (Thiagarajan et al., 2002). Therefore, the LTP/LTD induced in our system resembles that in the classical brain slice model. Furthermore, we have shown that the LTP/LTD is mediated by the NMDA receptors, as the antagonist of NMDA receptors blocked the light-induced LTP/LTD. The NMDA-dependent LTP/LTD is a cellular substrate of memory (Pare, 2004). Therefore, the NMDA-dependent LTP/LTD induced in our cultured human neural networks suggests that the human brain may use a very similar mechanism in processing information.

Our *in vitro* plasticity model is simple and versatile. We first developed the parameters using hESC-derived neurons, but the protocol is reproduced using iPSC-derived neurons. This is also reproduced when the lead authors moved to a new institution to set up a new laboratory. Although we chose cortical glutamate and GABA neurons to mimic cortical circuitry, one can use a combination of any other neural cell types to examine the transmission and plasticity. When these cells are from patient or disease stem cells, the model will enable assaying synaptic plasticity under psychiatric or neurological conditions, as shown by the defective LTP and LTD in DS iPSC-derived neuronal networks. It should be noted that the inability to induce LTP/LTD in the DS neuronal culture may also be associated with reduced synaptic activity (Weick et al., 2013). Nevertheless, our observation in DS patient iPSC-derived neuronal network is very similar to the deficit or even complete lack of LTP reported in hippocampal CA1 synapses of adult Ts65Dn mice, a model for DS (Costa and Grybko, 2005; Kleschevnikov et al., 2004; Siarey et al., 1997, 1999). Since our model is based on precise control of synaptic transmission by light and intracellular recording, it offers a new way to assess human neural plasticity at the single-synapse level when combined with engineering tools. Theoretically, such a model could provide a research platform for studying human learning and memory and building a computational model for circuit learning and memory.

Limitations of the Study

The LTP/LTD phenomena in the current paper are based on hESC-derived human neural networks. Although they are similar to those recorded in animal brain slices, they may involve different mechanisms, which requires further investigation.

METHODS

All methods can be found in the accompanying Transparent Methods supplemental file.

SUPPLEMENTAL INFORMATION

Supplemental Information can be found online at https://doi.org/10.1016/j.isci.2020.100829.

ACKNOWLEDGMENTS

This study was supported in part by the NIH-NIMH (MH099587, MH100031), NIH-NINDS (NS076352, NS086604), and the NICHD (HD076892, U54 HD090256). S.-C.Z. acknowledges the Steenbock Professorship. S.-C.Z. is co-founder of BrainXell, Inc.

AUTHOR CONTRIBUTIONS

S.-C.Z. and Y.D. designed the experiments and wrote the manuscript with input from M.X. and Y.C. Y.D. and M.X. processed the differentiation and histology experiments. Y.D. performed the electrophysiology experiments. Y.C. did the cell line construction experiments. Y.T. and X.L. helped with some of the experiments. Y.D. and M.X. collected and analyzed data. S.-C.Z. supervised the project.

DECLARATION OF INTERESTS

The authors declare no competing interests.

Received: October 17, 2019
Revised: December 24, 2019
Accepted: January 3, 2020
Published: February 21, 2020

REFERENCES

Bean, B.P. (2007). The action potential in mammalian central neurons. Nat. Rev. Neurosci. *8*, 451–465.

Beck, H., Goussakov, I.V., Lie, A.L., Helmstaedter, C., and Elger, C.E. (2000). Synaptic plasticity in the human dentate gyrus. J. Neurosci. *20*, 7080–7086.

Bliss, T.V., and Collingridge, G.L. (1993). A synaptic model of memory: long-term potentiation in the hippocampus. Nature *361*, 31–39.

Bliss, T.V., and Collingridge, G.L. (2013). Expression of NMDA receptor-dependent LTP in the hippocampus: bridging the divide. Mol. Brain *6*, 5.

Buonomano, D.V., and Merzenich, M.M. (1998). Cortical plasticity: from synapses to maps. Annu. Rev. Neurosci. *21*, 149–186.

Chen, H.X., Otmakhov, N., and Lisman, J. (1999). Requirements for LTP induction by pairing in hippocampal CA1 pyramidal cells. J. Neurophysiol. *82*, 526–532.

Chen, W., Hu, G.Y., Zhou, Y.D., and Wu, C.P. (1994). Two mechanisms underlying the induction of long-term potentiation in motor cortex of adult cat in vitro. Exp. Brain Res. *100*, 149–154.

Chen, W.R., Lee, S.H., Kato, K., Spencer, D.D., Shepherd, G.M., and Williamson, A. (1996). Long-term modifications of synaptic efficacy in the human inferior and middle temporal cortex. Proc. Natl. Acad. Sci. U S A *93*, 8011–8015.

Clapp, W.C., Kirk, I.J., Hamm, J.P., Shepherd, D., and Teyler, T.J. (2005). Induction of LTP in the human auditory cortex by sensory stimulation. Eur. J. Neurosci. *22*, 1135–1140.

Costa, A.C., and Grybko, M.J. (2005). Deficits in hippocampal CA1 LTP induced by TBS but not HFS in the Ts65Dn mouse: a model of Down syndrome. Neurosci. Lett. *382*, 317–322.

Dan, Y., and Poo, M.M. (2004). Spike timing-dependent plasticity of neural circuits. Neuron *44*, 23–30.

Daw, N., Rao, Y., Wang, X.F., Fischer, Q., and Yang, Y. (2004). LTP and LTD vary with layer in rodent visual cortex. Vis. Res. *44*, 3377–3380.

Ge, S., Goh, E.L., Sailor, K.A., Kitabatake, Y., Ming, G.L., and Song, H. (2006). GABA regulates synaptic integration of newly generated neurons in the adult brain. Nature *439*, 589–593.

Kim, K., Saneyoshi, T., Hosokawa, T., Okamoto, K., and Hayashi, Y. (2016). Interplay of enzymatic and structural functions of CaMKII in long-term potentiation. J. Neurochem. *139*, 959–972.

Kleschevnikov, A.M., Belichenko, P.V., Villar, A.J., Epstein, C.J., Malenka, R.C., and Mobley, W.C. (2004). Hippocampal long-term potentiation suppressed by increased inhibition in the Ts65Dn mouse, a genetic model of Down syndrome. J. Neurosci. *24*, 8153–8160.

Lee, H.K., and Kirkwood, A. (2011). AMPA receptor regulation during synaptic plasticity in hippocampus and neocortex. Semin. Cell Dev. Biol. *22*, 514–520.

Li, Y., Aimone, J.B., Xu, X., Callaway, E.M., and Gage, F.H. (2012). Development of GABAergic inputs controls the contribution of maturing neurons to the adult hippocampal network. Proc. Natl. Acad. Sci. U S A *109*, 4290–4295.

Li, Y., You, Q.L., Zhang, S.R., Huang, W.Y., Zou, W.J., Jie, W., Li, S.J., Liu, J.H., Lv, C.Y., Cong, J., et al. (2017). Satb2 ablation impairs hippocampus-based long-term spatial memory and short-term working memory and immediate early genes (IEGs)-Mediated hippocampal synaptic plasticity. Mol. Neurobiol. https://doi.org/10.1007/s12035-017-0531-5.

Li, X.J., Zhang, X., Johnson, M.A., Wang, Z.B., Lavaute, T., and Zhang, S.C. (2009). Coordination of sonic hedgehog and Wnt signaling determines ventral and dorsal telencephalic neuron types from human embryonic stem cells. Development *136*, 4055–4063.

Liu, X., Ramirez, S., Redondo, R.L., and Tonegawa, S. (2014). Identification and manipulation of memory engram cells. Cold Spring Harb. Symp. Quant. Biol. *79*, 59–65.

Liu, Y., Weick, J.P., Liu, H., Krencik, R., Zhang, X., Ma, L., Zhou, G.M., Ayala, M., and Zhang, S.C. (2013). Medial ganglionic eminence-like cells derived from human embryonic stem cells correct learning and memory deficits. Nat. Biotechnol. *31*, 440–447.

Lu, W., Man, H., Ju, W., Trimble, W.S., MacDonald, J.F., and Wang, Y.T. (2001). Activation of synaptic NMDA receptors induces membrane insertion of new AMPA receptors and

LTP in cultured hippocampal neurons. Neuron *29*, 243–254.

Malenka, R.C. (1994). Synaptic plasticity in the hippocampus: LTP and LTD. Cell *78*, 535–538.

Malenka, R.C., and Bear, M.F. (2004). LTP and LTD: an embarrassment of riches. Neuron *44*, 5–21.

Man, H.Y., Wang, Q., Lu, W.Y., Ju, W., Ahmadian, G., Liu, L., D'Souza, S., Wong, T.P., Taghibiglou, C., Lu, J., et al. (2003). Activation of PI3-kinase is required for AMPA receptor insertion during LTP of mEPSCs in cultured hippocampal neurons. Neuron *38*, 611–624.

Minatohara, K., Akiyoshi, M., and Okuno, H. (2015). Role of immediate-early genes in synaptic plasticity and neuronal ensembles underlying the memory trace. Front. Mol. Neurosci. *8*, 78.

Nabavi, S., Fox, R., Proulx, C.D., Lin, J.Y., Tsien, R.Y., and Malinow, R. (2014). Engineering a memory with LTD and LTP. Nature *511*, 348–352.

Nicoll, R.A. (2017). A brief history of long-term potentiation. Neuron *93*, 281–290.

Ninan, I., Liu, S., Rabinowitz, D., and Arancio, O. (2006). Early presynaptic changes during plasticity in cultured hippocampal neurons. EMBO J. *25*, 4361–4371.

Pare, D. (2004). Presynaptic induction and expression of NMDA-dependent LTP. Trends Neurosci. *27*, 440–441.

Siarey, R.J., Carlson, E.J., Epstein, C.J., Balbo, A., Rapoport, S.I., and Galdzicki, Z. (1999). Increased synaptic depression in the Ts65Dn mouse, a model for mental retardation in Down syndrome. Neuropharmacology *38*, 1917–1920.

Siarey, R.J., Stoll, J., Rapoport, S.I., and Galdzicki, Z. (1997). Altered long-term potentiation in the young and old Ts65Dn mouse, a model for Down Syndrome. Neuropharmacology *36*, 1549–1554.

Sidorov, M.S., Kaplan, E.S., Osterweil, E.K., Lindemann, L., and Bear, M.F. (2015). Metabotropic glutamate receptor signaling is required for NMDA receptor-dependent ocular dominance plasticity and LTD in visual cortex. Proc. Natl. Acad. Sci. U S A *112*, 12852–12857.

Sokolov, M.V., Rossokhin, A.V., M Kasyanov, A., Gasparini, S., Berretta, N., Cherubini, E., and Voronin, L.L. (2003). Associative mossy fibre LTP induced by pairing presynaptic stimulation with postsynaptic hyperpolarization of CA3 neurons in rat hippocampal slice. Eur. J. Neurosci. *17*, 1425–1437.

Steinbeck, J.A., Choi, S.J., Mrejeru, A., Ganat, Y., Deisseroth, K., Sulzer, D., Mosharov, E.V., and Studer, L. (2015). Optogenetics enables functional analysis of human embryonic stem cell-derived grafts in a Parkinson's disease model. Nat. Biotechnol. *33*, 204–209.

Suppa, A., Li Voti, P., Rocchi, L., Papazachariadis, O., and Berardelli, A. (2015). Early visuomotor integration processes induce LTP/LTD-like plasticity in the human motor cortex. Cereb. Cortex *25*, 703–712.

Tang, Y.P., Shimizu, E., Dube, G.R., Rampon, C., Kerchner, G.A., Zhuo, M., Liu, G., and Tsien, J.Z. (1999). Genetic enhancement of learning and memory in mice. Nature *401*, 63–69.

Teyler, T.J., Hamm, J.P., Clapp, W.C., Johnson, B.W., Corballis, M.C., and Kirk, I.J. (2005). Long-term potentiation of human visual evoked responses. Eur. J. Neurosci. *21*, 2045–2050.

Thiagarajan, T.C., Piedras-Renteria, E.S., and Tsien, R.W. (2002). alpha- and betaCaMKII. Inverse regulation by neuronal activity and opposing effects on synaptic strength. Neuron *36*, 1103–1114.

Weick, J.P., Held, D.L., Bonadurer, G.F., 3rd, Doers, M.E., Liu, Y., Maguire, C., Clark, A., Knackert, J.A., Molinarolo, K., Musser, M., et al. (2013). Deficits in human trisomy 21 iPSCs and neurons. Proc. Natl. Acad. Sci. U S A. *110*, 9962–9967.

Weick, J.P., Liu, Y., and Zhang, S.C. (2011). Human embryonic stem cell-derived neurons adopt and regulate the activity of an established neural network. Proc. Natl. Acad. Sci. U S A *108*, 20189–20194.

Zhou, Y., Won, J., Karlsson, M.G., Zhou, M., Rogerson, T., Balaji, J., Neve, R., Poirazi, P., and Silva, A.J. (2009). CREB regulates excitability and the allocation of memory to subsets of neurons in the amygdala. Nat. Neurosci. *12*, 1438–1443.

iScience, Volume *23*

Supplemental Information

Plasticity of Synaptic Transmission in Human Stem Cell-Derived Neural Networks

Yi Dong, Man Xiong, Yuejun Chen, Yezheng Tao, Xiang Li, Anita Bhattacharyya, and Su-Chun Zhang

Transparent Methods

Construction of donor plasmid.

To generate AAVS1-pur-CAG-ChR2 (H134R)-EYFP donor plasmid, we amplified ChR2 (H134R)-EYFP cDNA by PCR from pAAV-hSyn-hChR2 (H134R)-EYFP (Addgene #26973). The ChR2 (H134R)-EYFP fragment was inserted into the AAVS1-pur-CAG-EGFP donor plasmid (Chen et al., 2016) to replace EGFP, generating the AAVS1-pur-CAG-ChR2 (H134R)-EYFP donor plasmid. Human codon-optimized wild type Cas9 (Cas9-2A-EGFP) and sgRNA T2 plasmids were obtained from Addgene (#44719, #41818) (Ding et al., 2013; Mali et al., 2013).

Generation of ChR2 (H134R)-EYFP expressing hESC and iPSC lines.

H9 hESCs were obtained from WiCell (line WA09, passages 20–40). The Down Syndrome (DS) iPSCs (UWWC1-DS1, trisomy 21) and isogenic control iPSCs (UWWC1-DS2U, euploid) was generated from mosaic fibroblasts of a Down syndrome patient (Weick et al., 2013). hESCs or iPSCs were pretreated by Rho Kinase (ROCK)-inhibitor (0.5 μM, Calbiochem, H-1152P) overnight. After disaggregation of hESCs or iPSCs by TrypleLE^{TM} (Life Technology), cells were dispersed into single cells and resuspended in the Electroporation Buffer (KCl 5 mM, $MgCl_2$ 5 mM, HEPES 15 mM, Na_2HPO_4 102.94 mM, NaH_2PO_4 47.06 mM, PH = 7.2) with 15 μg Cas9 plasmid, 15 μg sgRNA T2 plasmid, and 30 μg AAVS1-pur-CAG-ChR2 (H134R)-EYFP donor plasmid. Electroporation was carried out using the Gene Pulser Xcell System (Bio-Rad). Cells were subsequently plated and selected by

puromycin (0.5 μg/ml, Invivogen, ant-pr-1) for two weeks on the mouse embryonic fibroblast (MEF) feeder. Individual colonies were picked up and identified by genomic PCR.

Generation of glutamate neurons and GABA neurons from hESCs.

The procedure for generating glutamate or GABA neurons from hESCs was described previously (Li et al., 2009; Liu et al., 2013). ChR2-EYFP cells or H9 (passages 25–35) ESCs as well as ChR2-EYFP DS or isogenic iPSCs were cultured on a feeder layer with a daily change of medium for 1 week. Then, ESC colonies were detached from the feeder layer and grown in the ESC medium for 4 days to help form cell aggregates. For neural induction, cell aggregates were cultured with the Neural Induction Medium (NIM) (DMED/F12, 1% N2, 1% MEM NEAA, Life Technologies) supplemented with 2uM SB431542 (Stemgent), 2 uM DMH1 (Torcris) for additional 3 days. The ESC aggregates were then adhered to 6-well plates in NIM (plus 5%FBS) for 20h followed by another 2 days with the NIM from day4-7. By 10 days after ESC differentiation, neuroepithelial cells appeared in the form of rosettes. For glutamate neuron differentiation, the neuroepithelial cells were cultured in the NIM till neural tube-like rosettes formed at around day 16, which were gently blown off by a 1-ml pipette and suspended in the same medium for another 2 weeks. To induce GABA progenitors, the neuroepithelial cells were treated with SAG (sonic hedgehog agonist, 1 μM, Calbiochem) from d 10 till d 26.

For co-culture, the ChR2-EYFP glutamate neuronal progenitors and non-ChR2 GABA progenitors (day-26) were mixed by 2:1 under the neuron maturation medium (neural basal medium containing 1% N2 (Life Technologies), 2% B27 (LifeTechnologies), brain-derived neurotrophic factor (10 ng/ml, PeproTech), glial cell line derived neurotrophic factor (10 ng/ml, PeproTech), ascorbic acid (200 μM,

Sigma-Aldrich), cAMP (1 μM, Sigma-Aldrich), insulin-like growth factor I (PeproTech,10 ng/ml), Compound E (1 μM, Calbiochem, for 1 week after attachment) and glutamax (1:1000, Life technologies) for up to 5 weeks before whole-cell patch-clamp recordings

Immunochemical staining.

Immunostaining of coverslip co-cultures was performed as previously described (Chen et al., 2016). Briefly, neurons on coverslips were fixed in 4% paraformaldehyde for 30min and rinsed with PBS 3 times. Coverslips were incubated in a blocking buffer for 1 hour followed by primary antibodies (Goat GFP, Abcam, 1:1000; Rb GABA, sigma, 1:5000; Mouse monoclonal GFAP, Millipore, 1:1000) overnight at 4℃. Coverslips were incubated for 1 h at room temperature with fluorescently conjugated secondary antibodies (Invitrogen). The nuclei were stained with Hoechst 33258. Images were collected with a Nikon A1R-Si laser-scanning confocal microscope (Nikon, Tokyo, Japan).

Electrophysiology and ChR2 stimulation.

The cultured cells were continuously perfused with artificial cerebrospinal fluid (ACSF) saturated with 95% O_2/5% CO_2. The composition of ACSF was (in mM) 124 NaCl, 3.5 KCl, 1.5 $CaCl_2$, 1.3 $MgSO_4$, 1.24 KH_2PO_4, 18 $NaHCO_3$, 20 glucose, PH 7.4. Electrodes (Sutter instrument) were pulled from glass capillaries using a Sutter instrument puller (model P-97). The electrodes were filled with a inner solution consisting of (in mM) 140 K-gluconate, 0.1 $CaCl_2$, 2 $MgCl_2$, 1 EGTA, 2 ATP K_2, 0.1

GTP Na_3, and 10 HEPES, PH 7.25 (290 mOsm) and had a resistance of 4-6 MΩ. Whole-cell voltage-clamp and current-clamp recordings were carried out at 30 ˚C. Neurons were visualized using an Olympus Optical (Tokyo, Japan) BX51WI microscope with differential interference contrast optics at 40X. Voltage and current clamp recordings were obtained using a MultiClamp 700B amplifier (Axon instruments). Signals were filtered at 4 kHz using a Digidata 1322A analog-to-digital converter (Axon instruments). Access resistance was observed prior to and following recordings and neurons with resistances > 25 MΩ at either point were discarded from analyses. Series resistance was compensated > 60% except in post-synaptic current (PSC) recording where it was not compensated.

To observe paired pulse facilitation (PPF), two synaptic responses were evoked by a pair of stimuli (5 ms pulse) given at short intervals (50 ms) at 0.05 Hz, PPF ratio is the ratio of the second eEPSC amplitude to the first, or P2/P1. Miniature EPSCs (mEPSCs) were recorded in sweeps of 2 s at a holding potential of -70 mV under the voltage clamp mode in the presence of tetrodotoxin (TTX; 0.5 μM) and picrotoxin (50 μM) to block voltage-dependent sodium channels and $GABA_A$ receptors, respectively.

A light stimulation fiber was placed 5mm from the dish and picrotoxin (50 μM) was included in ACSF to block $GABA_A$ receptors. Light stimulation was achieved by a custom-made LED device (1 Watt, 470 nm; Cree lighting Inc.) coupled to a fiber optic cable. A National Instruments USB-6501 DAQ provided the trigger pulses, with timing controlled by pClamp (Axon). The light-evoked EPSCs (eEPSCs) were elicited by

0.05 Hz under the voltage-clamp mode. After at least a 5 min baseline eEPSC collection, LTP of unitary eEPSCs was induced by 200 ms light stimulation pairing with postsynaptic depolarization (voltage step to 0 mV, 200 ms) under the current-clamp mode. Pairing was repeated 20 times at 0.1 Hz. For LTD induction, we applied low frequency stimulation (LFS, 900 pulse, 3 Hz) by blue light.

Calcium imaging.

Coverslip cultures were loaded with the calcium-sensitive fluorescent dye Quest Rhod-4 AM (10 μM) for 15 min at 37 °C (Lock et al., 2015). The fluorescence intensity was measured at 549 nm in response to 578 nm excitation and the fluorescence increase upon binding Ca^{2+} with little shift in wavelength. The data use the time points just before and after the light stimulation. The Ca^{2+} concentration was analyzed using intergrated optical density (IOD), which reflects a relative, not an absolute measurement of the free Ca^{2+} concentration. Images were collected with a Nikon A1R-Si laser-scanning confocal microscope (Nikon, Tokyo, Japan).

Single cell harvesting and in-tube reverse transcription.

Cell harvesting was performed according to the previous published paper (Fuzik et al., 2016). At the end of induction of LTP or LTD, the pipette was clamped to −5 mV (Vhold) and then a continuous series of depolarizing rectangular voltage pulses (5 ms at 5 ms intervals) were applied for 6 min with amplitudes of 25 mV from Vhold. One hour after that, we aspirated cell body with all the intracellular

components into the pipette tips with a minimal negative pressure. All the contents (about 0.5 µl) in the tip was ejected into freshly prepared 4.5 µl lysis buffer (0.25% NP40, 2.3 mM DTT, 0.4 U/µl RNAse inhibitor, and 1 µM OL(dT)30 Primer) in a 200 µl EP tube and stored at -80°C until batch processing. After all the samples were collected, the in-tube reverse transcription and amplification were performed as previously described with minor modification (Picelli et al., 2014). The samples were thawed and incubated at 70 °C for 3 min, then cooled to 4 °C. 5 µl reverse transcription buffer containing 0.7 mM dNTP, 1 µM TSO primer, 0.8 U/ µl RNAse inhibitor, and 1 U/ µl SMartase was added and incubated at 42 °C for 90 min followed by 70 °C for 10 min. The products of the reverse transcription were mixed with PCR buffer (1X EX Taq buffer, 0.4 mM dNTP, 0.4 µM IS PCR primer, and 0.05 U/µl TaKaRa EX Taq hot start) and amplified using thermal cycling 95 °C for 1 min (1 cycles), 95 °C 30 s, 65 °C 30 s, 72 °C 8 min (12 cycles). All the samples (cDNA) then underwent purification by AMPure XP beads (Beckman coulter). The Ct of GAPDH of all the samples was between 17-23.

Quantitative real time PCR.

Quantitative real time PCR was performed on CFX RT-PCR detection system (BioRad) using the iTaq SYBR green supermix (BioRad) according to the manufacturer's instructions. To determine the relative expression levels of different genes, ΔCt (Ct GAPDH-Ct gene) was calculated and normalized to the control cells (without laser, group LTP and LTD). Primers are listed in Table S1.

Statistical analysis.

All data were obtained from independent coverslip cultures. Offline data analysis was performed using MiniAnalysis software (Synaptosoft), Clampfit 9.0 (Axon) and origin (Origin). All data were presented as the mean ± SEM and significance was determined using the paired Student's t-test, one-way ANOVA, or two-way ANOVA.

Supplemental References

Chen, Y., Xiong, M., Dong, Y., Haberman, A., Cao, J., Liu, H., Zhou, W., and Zhang, S.C. (2016). Chemical Control of Grafted Human PSC-Derived Neurons in a Mouse Model of Parkinson's Disease. Cell Stem Cell.

Ding, Q., Regan, S.N., Xia, Y., Oostrom, L.A., Cowan, C.A., and Musunuru, K. (2013). Enhanced efficiency of human pluripotent stem cell genome editing through replacing TALENs with CRISPRs. Cell Stem Cell *12*, 393-394.

Fuzik, J., Zeisel, A., Mate, Z., Calvigioni, D., Yanagawa, Y., Szabo, G., Linnarsson, S., and Harkany, T. (2016). Integration of electrophysiological recordings with single-cell RNA-seq data identifies neuronal subtypes. Nat Biotechnol *34*, 175-183.

Li, X.J., Zhang, X., Johnson, M.A., Wang, Z.B., Lavaute, T., and Zhang, S.C. (2009). Coordination of sonic hedgehog and Wnt signaling determines ventral and dorsal telencephalic neuron types from human embryonic stem cells. Development *136*, 4055-4063.

Liu, Y., Weick, J.P., Liu, H., Krencik, R., Zhang, X., Ma, L., Zhou, G.M., Ayala, M., and Zhang, S.C. (2013). Medial ganglionic eminence-like cells derived from human embryonic stem cells correct learning and memory deficits. Nat Biotechnol *31*, 440-447.

Lock, J.T., Parker, I., and Smith, I.F. (2015). A comparison of fluorescent Ca(2)(+) indicators for imaging local Ca(2)(+) signals in cultured cells. Cell calcium *58*, 638-648.

Mali, P., Yang, L., Esvelt, K.M., Aach, J., Guell, M., DiCarlo, J.E., Norville, J.E., and Church, G.M. (2013). RNA-guided human genome engineering via Cas9. Science *339*, 823-826.

Picelli, S., Faridani, O.R., Bjorklund, A.K., Winberg, G., Sagasser, S., and Sandberg, R. (2014). Full-length RNA-seq from single cells using Smart-seq2. Nat Protoc *9*, 171-181.

Weick, J.P., Held, D.L., Bonadurer, G.F., 3rd, Doers, M.E., Liu, Y., Maguire, C., Clark, A., Knackert, J.A., Molinarolo, K., Musser, M., *et al.* (2013). Deficits in human trisomy 21 iPSCs and neurons. Proc Natl Acad Sci U S A *110*, 9962-9967.

Figure S1. Related to Figure 1

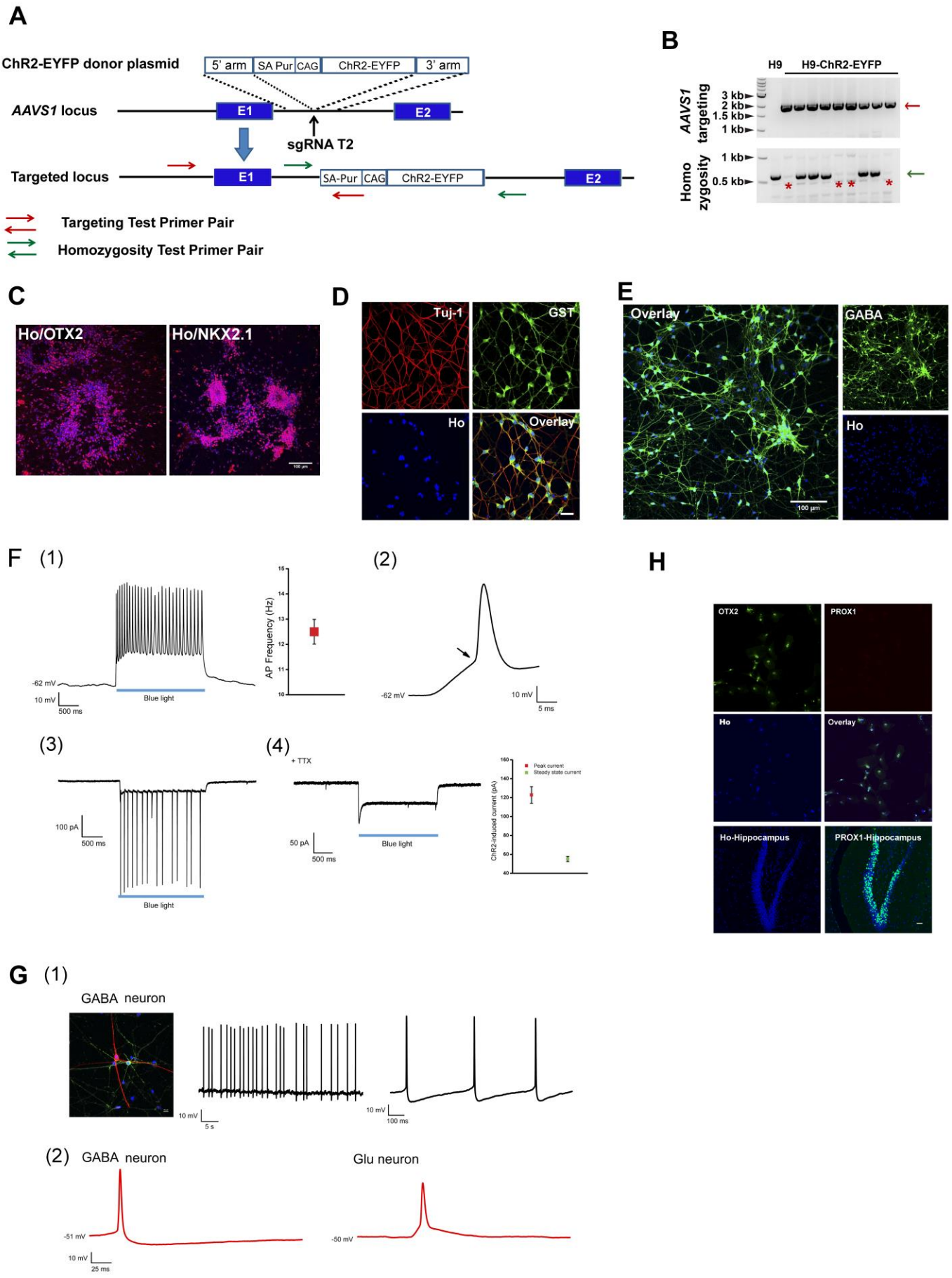

Figure S1. Establishment of ChR2-expressing hESCs and neural differentiation. A. Schematic diagram showing the strategy for knock-in of ChR2-EYFP-expressing cassette into the AAVS1 locus. Exons are shown as blue boxes. The vertical arrows indicate targeting site by sgRNA T2 in AAVS1 locus. SA-Pur, splice acceptor sequence followed by a T2A self-cleaving peptide sequence and the puromycin resistance gene. CAG, synthetic CAGGS promoter. EYFP is fused to the C terminus of ChR2. PCR primers for AAVS1 locus insertion or homozygosity are indicated as red arrows and green arrows, respectively. B. PCR genotyping of ChR2-EYFP-expressing hESC clones. Red arrow indicates the expected PCR products (~2000bp) for correctly targeted AAVS1 locus. Green arrow indicates the PCR products (~650bp) of heterozygous clones. Red asterisks indicate the homozygous clones without PCR products. C. Immunostaining of the co-cultured progenitors. Almost all cells were stained by OTX2 and NKX2.1, indicating ventral forebrain identity. D. Immunocytochemistry analysis of hESC-derived ChR2-expressing glutamate neurons. The efficiency for directing ChR2-expressing hESCs into glutamatergic neurons is 92.9 ± 3.3 % based on expression of glutamine synthase (GST) (n = 5 different differentiation cultures). Ho, Hoechst. Scale bar, 25 μm. E. Immunocytochemistry analysis of hESC-derived GABAergic neurons. The efficiency for directing hESCs into GABAergic neurons is 81.9 ± 2.3 % based on expression of GABA (n = 5 different differentiation cultures). Ho, Hoechst. Scale bar, 25 μm. F. Light-induced action potentials and currents in ChR2-expressing hESC-derived glutamatergic neurons. (1) Left: Representative traces from current-clamp recordings of a ChR2+ cell during a 2 s, 470nm light stimulus. Right: The averaged frequency of APs (n = 7). (2) Expanded timescale of current-clamp recording demonstrates the presence of action potentials by a clear threshold deflection (arrow). (3) Representative traces from voltage-clamp recordings of a ChR2+ cell during a 2 s, 470nm light stimulus. (4) Left: ChR2-induced inward currents in the presence of 1 μM Tetrodotoxin (TTX). Right: the averaged amplitude of the two components of ChR2-induced currents (n = 7). G. Difference of action potentials between glutamatergic neurons and GABA neurons. (1) Left, neurobiotin staining of recorded GABAergic neurons (Red: GABA neuron;

Green: ChR2-expressing neuron). Middle, spontaneous action potentials in an hESC-derived GABA neuron. Right, expanded timescale of the spontaneous action potentials in an hESC-derived GABA neuron. (2) Left, action potential in an hESC-derived GABA neuron. Right, action potential in an hESC-derived glutamatergic neuron. H. Immunofluorescence images of co-cultured neurons immunostained for OTX2, PROX1, Ho as well as immunofluorescence images of hippocampus immunostained for PROX1, Ho (Bottom panel). Ho, Hoechst. Scale bar, 100 μm.

Figure S2. Related to Figure 2 and Figure 3

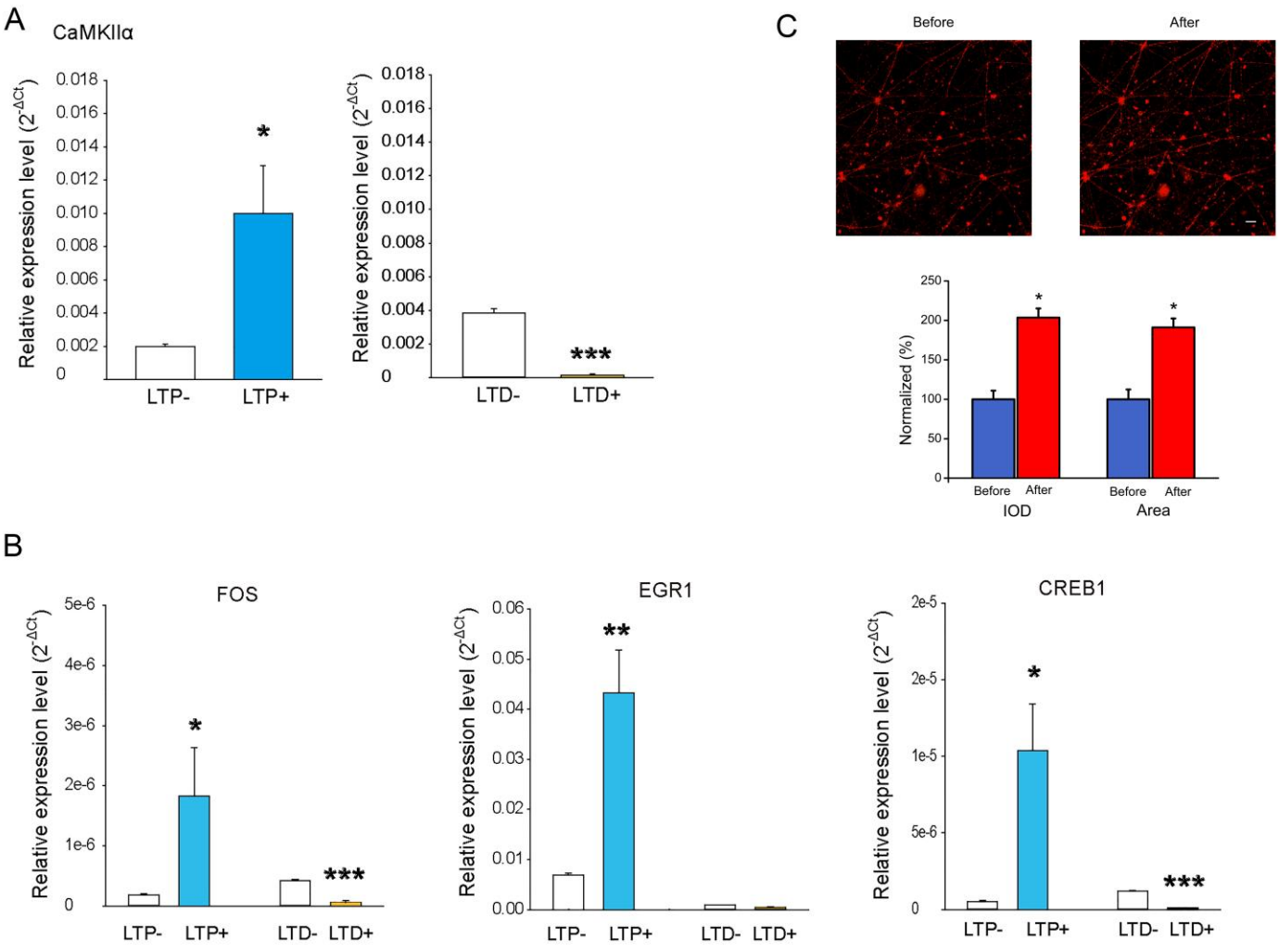

Figure S2. The molecular changes in postsynaptic cells after LTP or LTD induction. A. The expression changes of CAMKIIA in the postsynaptic neurons after LTP or LTD induction. The relative expression levels of CAMKIIA after LTP (Left) and LTD (Right) induction were shown in $2^{-\Delta Ct}$. $\Delta Ct = Ct_{GAPDH} - Ct_{gene}$. 4 cells in each group. * P < 0.05, ** P < 0.01, ***P<0.001; t-test. B. The expression changes of IEGs in the postsynaptic neurons after LTP or LTD induction. The relative expression levels of IEGs FOS (Left), EGR1 (Middle), and CREB1 (Right) after LTP and LTD induction were shown in $2^{-\Delta Ct}$. $\Delta Ct = Ct_{GAPDH} - Ct_{gene}$. 4 cells in each group. * P < 0.05, ** P<0.01, ***P < 0.001; t-test. C. Effect of light stimulation on calcium influx in co-cultured neurons. Scale bar, 100 μm. n= 4, P < 0.001, t-test.

Table S1 Related to Figure 2 and Figure 3. Primers for qPCR

Gene	5’ primer	3’ primer
GAPDH	GCACCGTCAAGGCTGAGAAC	AGGGATCTCGCTCCTGGAA
CAMK2A	ACCACTACCTGATCTTCGACC	CCGCCTCACTGTAATACTCCC
FOS	CCGGGGATAGCCTCTCTTACT	CCAGGTCCGTGCAGAAGTC
EGR1	GGTCAGTGGCCTAGTGAGC	GTGCCGCTGAGTAAATGGGA
CREB1	ATTCACAGGAGTCAGTGGATAGT	CACCGTTACAGTGGTGATGG